Journal of Modern Optics

ISSN: 0950-0340 (Print) 1362-3044 (Online) Journal homepage: https://www.tandfonline.com/loi/tmop20

Anatomy of strong field ionization

Misha Yu Ivanov , Michael Spanner & Olga Smirnova

To cite this article: Misha Yu Ivanov , Michael Spanner & Olga Smirnova (2005) Anatomy of strong field ionization, Journal of Modern Optics, 52:2-3, 165-184, DOI: 10.1080/0950034042000275360

To link to this article: https://doi.org/10.1080/0950034042000275360

Published online: 02 Sep 2006.

JOURNAL OF MODERN OPTICS, 20 JANUARY–15 FEBRUARY 2005
VOL. 52, NO. 2–3, 165–184

Taylor & Francis
Taylor & Francis Group

Anatomy of strong field ionization*

MISHA YU IVANOV†, MICHAEL SPANNER‡
and OLGA SMIRNOVA§

†National Research Council of Canada, 100 Sussex Drive,
Ottawa, Ontario K1A 0R6, Canada; e-mail: misha.ivanov@nrc.ca
‡Department of Physics, University of Waterloo,
Ontario N2L 3G1, Canada
§Photonics Institute, Vienna University of Technology,
Gusshausstrasse 27/387, A-1040 Vienna, Austria

(*Received 5 May 2004*)

Abstract. Strong field ionization is a starting point for a rich set of physical phenomena associated with attosecond science. This paper provides an introductory overview of the basic theory of strong field ionization and focuses on (i) the physics and the dynamics of the electron transition to the continuum, and (ii) the shape of the electron wavepacket as it appears in the continuum.

1. Introduction

The purpose of this introductory overview is three-fold. Firstly, it is supposed to provide a reasonably easy-to-read primer into the theory of strong field ionization, known as the 'Strong Field Approximation' (SFA). Strong field ionization is a starting point for a rich set of physical phenomena associated with the new field of attosecond science; it is useful to have a clear review of the basics of its theory. We have tried to present these basics as simply as possible and to list most of the warnings one has to have in mind using SFA.

Secondly, this review serves as a vehicle to put forward our perspective on the dynamics of strong field ionization, specifically on how multiphoton and tunnel ionization in strong laser fields co-exist. Along the way, we have tried to argue why the SFA works so well for noble atoms and sufficiently low laser frequencies.

Thirdly, we look in some detail at the shape of the electronic wavepacket as it emerges from the potential well and appears in the continuum. This seemingly academic question has important consequences when trying to simulate classically or semi-classically the strong field dynamics that follows ionization.

When a laser field interacting with an atom or a molecule is weak, conventional time-dependent perturbation theory allows us to understand and describe almost everything. But what do you do when the perturbation theory is no longer applicable, which is definitely the case in strong field ionization? Clearly, the laser field should be included as fully as possible. In principle, one can give up and resort to numerical simulations. However, dealing with atomic or molecular dynamics in strong laser fields, one has to face a situation where the energy of

*Reviewing of this paper was handled by a member of the Editorial Board.

Journal of Modern Optics ISSN 0950–0340 print/ISSN 1362–3044 online © 2005 Taylor & Francis Ltd
http://www.tandf.co.uk/journals
DOI: 10.1080/0950034042000275360

the system and the strength of the interaction can change by $\sim 100\,\text{eV}$ within a fraction of a femtosecond. Fitting such simulations within a reasonable computer time and memory is exceptionally challenging and requires good understanding of the physics of the problem. This is where approximate analytical theories are indispensable, even when the approximations are justified not as much by rigorous math as by physical reasoning.

Nine times out of ten perturbation theory of one sort or another is the only approach that is technically tractable. Fortunately, in strong fields an alternative perturbation theory seems reasonable: if the field is strong, why don't we include it exactly and treat the potential of the field-free system as a perturbation? this is the idea behind the Strong Field Approximation (SFA) pioneered by Keldysh, Reiss and Faisal [1–3]. The SFA has so many flaws that fly right into the face of a rigorous quantum theory that it is amazing how its early version was published in such a puritan (at that time) Russian journal as JETP [1]. But SFA works for getting the basic physics right and that is what counts in the end. Here we focus on the early part of ionization dynamics: how the electron appears in the continuum. We review the formalism, the main approximations and their drawbacks, show how and why multiphoton ionization and tunneling co-exist and finally look at the anatomy of the electronic wavepacket as it tunnels out of the potential well into the continuum.

2. Basic formalism and S-matrix amplitudes

The time-dependent Schroedinger equation (atomic units are used everywhere)

$$i\frac{\partial}{\partial t}|\Psi\rangle = \hat{H}(t)|\Psi\rangle \tag{1}$$

has a formal solution

$$|\Psi(t)\rangle = e^{-i\int_0^t \hat{H}(t')\,\mathrm{d}t'}|\Psi(t=0)\rangle = e^{-i\int_0^t \hat{H}(t')\,\mathrm{d}t'}|\Phi_\mathrm{i}\rangle. \tag{2}$$

The exponential operator $\exp[-i\int_0^t \hat{H}(t')\,dt']$ is the propagator and $|\Phi_\mathrm{i}\rangle$ is the initial state of the system at the initial moment set here at $t = 0$.

As is, this formal solution is of little use: evaluating exponential operators is a tedious task. A common denominator behind various SFA-type theories is the attempt to find a way to deal with this operator, using physical insight as one of the key inputs. In the end, the goal is to substitute the operator $\exp[-i\int^t \hat{H}(t')\,\mathrm{d}t']$ with a number $\exp[-i\int^t E(t')\,\mathrm{d}t']$, where $E(t)$ is some energy. Of course, such substitutions are not generally correct because different spatial parts of the initial wavefunction will evolve differently (with different energies): think about trajectories starting at different points in space.

The SFA is based on the observation that the desired substitution can be made rigorously for a free electron, in the presence of an arbitrarily polarized laser field: the force exerted by the laser field is the same everywhere (dipole approximation), the accumulated phase is coordinate-independent.

Let us partition the Hamiltonian $\hat{H}$ into two parts: $\hat{H} = \hat{H}_0 + \hat{V}$. *One may select these two pieces any way one wants, and the resulting expressions would all be mathematically equivalent*. The black art of making the partition is in getting expressions which are (i) reasonably simple, (ii) physically transparent and

consistent with the physical picture of the process (iii) well suited for reasonable approximations that make physical sense. Here we select $\hat{H}_0$ to be the field-free Hamiltonian of the quantum system and $\hat{V}_{\rm L}(t)$ is the interaction with the laser field, which we take in the length gauge $\hat{V}_{\rm L}(t) = -\mathbf{d}\mathbf{F}(t)$, $\mathbf{d}$ being the dipole moment of the system and $\mathbf{F}$ being the strength of the electric field, bold font means 'vector'.

Having chosen the partition, one can check by direct substitution that

$$|\Psi(t)\rangle = -i\int_0^t dt' \left[e^{-i\int_{t'}^{t}\hat{H}(t'')\,dt''}\right]\hat{V}_{\rm L}(t')\left[e^{-i\int_0^{t'}\hat{H}_0(t'')\,dt''}\right]\times$$
$$\times\,|\Phi_{\rm i}\rangle + e^{-i\int_0^t \hat{H}_0(t'')\,dt''}|\Phi_{\rm i}\rangle \tag{3}$$

is the exact solution of equation (1). The role of the second term in equation (3) is to ensure that the initial condition $|\Psi(t=0)\rangle = |\Phi_{\rm i}\rangle$ is satisfied. This second term is often forgotten, as *for this particular partition* it amounts to benign evolution of the initially bound state under the field-free Hamiltonian, contributing nothing to ionization. One should keep in mind, however, that other partitions could make this term important.

To simplify things a little bit, let us project $|\Psi(t)\rangle$ onto some final state of interest, such as a continuum state characterized by the electron velocity $\mathbf{v}$. The corresponding amplitude $a_{\mathbf{v}}(t)$ of populating the velocity $\mathbf{v}$ at the moment t is

$$a_{\mathbf{v}}(t) = -i\int_0^t dt' \langle\mathbf{v}|\left[e^{-i\int_{t'}^{t}\hat{H}(t'')\,dt''}\right]V_{\rm L}(t')\left[e^{-i\int_0^{t'}\hat{H}_0\,dt''}\right]|\Phi_{\rm i}\rangle. \tag{4}$$

The second (field-free) term in equation (4) is now gone—our assumption is that there was no initial population in the continuum. Note that here $|\mathbf{v}\rangle$ is not a plane wave but the exact outgoing continuum state which becomes the plane wave $\exp(i\mathbf{v}\mathbf{x})$ as $|\mathbf{x}| \to \infty$.

Equation (4), known as the time-reversed S-matrix amplitude, does not look very inviting. So far all we have managed to do is to replace an already complicated exponential operator with an even more sinister-looking integral, with two exponential operators in it. However, it is in this general, and exact, expression where interesting approximations can be explicitly tried, based almost exclusively on physical reasoning.

3. The Volkov propagator and the strong field approximation

Let us think about the physics of the situation in a strong low-frequency field. 'Low' means 'compared with the characteristic response frequency' of the system. While the electron is in the ground state, it follows slow (from the electron's perspective) oscillations of the laser field: the laser field polarizes the electron cloud. Not much else is happening until the electron manages to escape to the continuum, or to the manifold of highly excited states which do not look much different from the continuum in these strong laser fields. Escape can happen at any instant t'. Once the electron comes out of the deeply bound ground state, the strong field takes over and the electron starts to oscillate in the field, possibly scattering on the parent ion. Can we put this physical picture into mathematical terms? or, rather, can we use this picture to do something to the formal expressions for the amplitude $a_{\mathbf{v}}$?

Let us now look at the time-reversed S-matrix amplitude equation (4). Starting in $|\Phi_i\rangle$, the system is hit by a sequence of three operators: two exponential operators in the square brackets in equation (4) and the operator $\hat{V}_L$. The two exponential operators are the propagators from $t = 0$ to t' and from t' to t. The first propagator is field-free: during the time interval before t' our system sits in the ground state, oblivious to the laser field, accumulating the phase due to its energy $\exp(-iE_i t') = \exp(iI_p t')$ where I_p is the ionization potential. Procrastination ends at t' when the system is kicked by the instantaneous laser field $\hat{V}_L(t')$. To which state the transition occurs at this moment is anybody's guess. It is a virtual transition that can go anywhere—the energy conservation law need not be satisfied until the interaction is over. Then, from the moment t' to the moment of observation t the evolution proceeds under the action of the full Hamiltonian $\hat{H}$, including both the laser field and the field-free potential. Naturally, we integrate over all possible instants t' at which the system 'wakes up' and discovers that there is a strong laser field around.

The similarity of the physical picture suggested by our intuition (first paragraph of this section) and the time-reversed S-matrix expression equation (4) (second paragraph) is obvious. Equation (4) appears perfectly suited for using this physical picture for making reasonable approximations. What would these be?

While in the continuum, the electron is dominated by the laser field. Therefore, instead of the exact propagator $\exp(-i\int_{t'}^{t}\hat{H}\,dt'')$ we will use an approximate propagator $\exp(-i\int_{t'}^{t}\hat{H}_F\,dt'')$ which includes the laser field fully and exactly but completely ignores the field-free binding potential of the system $\hat{V}_A$: $\hat{H}_F \equiv \hat{H} - \hat{V}_A$. This approximation is the essence of SFA. One of the main reasons to completely neglect the atomic (or molecular) potential in the continuum is that the propagator for the free electron in the laser field, the Volkov propagator, is known analytically. Before writing it down, let us think about the physics again.

If the free electron shows up in the continuum at an instant t' with velocity $\mathbf{v}'$, then its velocity $\mathbf{v}$ at any later time t is

$$\mathbf{v} = \mathbf{v}' + \frac{q}{m}\mathbf{A}(t') - \frac{q}{m}\mathbf{A}(t), \tag{5}$$

where q and m are the electron charge and mass and $\mathbf{A}(t)$ is the vector-potential of the electric field defined as

$$\mathbf{F}(t) = -\frac{\partial \mathbf{A}(t)}{\partial t} \tag{6}$$

(As a side note, let us mention that, for very short laser pulses which include only few laser cycles, say one or two, the pulse envelope may change significantly over one laser period. In such cases one should define the vector-potential first and then use equation (6) to find the electric field.) Setting $q/m = -1$, we have

$$\mathbf{v} = \mathbf{v}' - \mathbf{A}(t') + \mathbf{A}(t). \tag{7}$$

The conserved quantity $\mathbf{P} = \mathbf{v}(t) - \mathbf{A}(t)$ is called the canonical momentum. The instantaneous energy during oscillations $E(t) = 1/2[\mathbf{v}' - \mathbf{A}(t') + \mathbf{A}(t)]^2$ is independent of where the electron is. The Volkov propagator $\exp(-i\int \hat{H}_F\,dt'')$, not surprisingly, is

$$e^{-i\int_{t'}^{t}\hat{H}_F(t'')\,dt''}|\mathbf{v}'\rangle = e^{-i\int_{t'}^{t}E(t'')\,dt''}|\mathbf{v}\rangle, \tag{8}$$

or

$$\langle \mathbf{v}|\, e^{-i\int_{t'}^{t} \hat{\boldsymbol{H}}_{\mathrm{F}}(t'')\,\mathrm{d}t''} = e^{-i\int_{t'}^{t} E(t'')\,\mathrm{d}t''} \langle \mathbf{v}'|. \tag{9}$$

Now $|\mathbf{v}'\rangle$ *and* $|\mathbf{v}\rangle$ *are the plane waves*. They have different velocities related by equation (7). The temporal phase added is the same for all coordinates because the laser field is homogeneous. Note that the propagation changes the coordinate part of the wavefunction between $|\mathbf{v}'\rangle$ and $|\mathbf{v}\rangle$, but in the exact same way for all coordinates. If we specify the final velocity $\mathbf{v}$ which the electron should have at the moment of observation t, then we know that, at the moment t', the moment of 'birth' in the continuum, the electron must show up in the state $|\mathbf{v}'\rangle = |\mathbf{v} + \mathbf{A}(t') - \mathbf{A}(t)\rangle$. At any other instant t'' between the moment of birth t' and the moment of observation t the instantaneous velocity and the energy are $\mathbf{v}(t'') = \mathbf{v} + \mathbf{A}(t'') - \mathbf{A}(t)$ and $E(t'') = 1/2[\mathbf{v} + \mathbf{A}(t'') - \mathbf{A}(t)]^2$. This is the energy in equations (8) and (9).

We can now write the SFA approximate expression for the amplitude equation (4). The system starts in the ground state $|\Phi_{\mathrm{i}}\rangle = |g\rangle$ with the energy $-I_{\mathrm{p}}$, and hence the phase $\exp(+iI_{\mathrm{p}}t')$ accumulated before discovering the laser field at t' replaces the first exponential operator. Replacing $\hat{\boldsymbol{H}}$ with $\hat{\boldsymbol{H}}_{\mathrm{F}}$ changes the second exponential operator into a simple phase as well:

$$\Psi(\mathbf{v}, t) = -i\int_0^t \mathrm{d}t'\, e^{-i(1/2)\int_{t'}^{t}[\mathbf{v}+\mathbf{A}(t'')-\mathbf{A}(t)]^2\,\mathrm{d}t''} \langle \mathbf{v} + \mathbf{A}(t') - \mathbf{A}(t)|\, V_{\mathrm{L}}(t')|g\rangle e^{+iI_{\mathrm{p}}t'}. \tag{10}$$

We have changed the notation from $a_{\mathbf{v}}(t)$ to $\Psi(\mathbf{v}, t)$ because now $|\mathbf{v}\rangle$ is a plane wave and $\langle \mathbf{v}|\Psi(t)\rangle$ is the velocity-domain representation of $|\Psi(t)\rangle$.

Equation (10) is very intuitive and is sketched in figure 1. The electron sits in the ground state until t' and accumulates a phase $\exp(iI_{\mathrm{p}}t')$. At instant t' it is kicked by the laser field into the continuum, to the state with instantaneous velocity $\mathbf{v}' = \mathbf{v} + \mathbf{A}(t') - \mathbf{A}(t)$ which is dictated by the velocity $\mathbf{v}$ at the moment of observation. Then the electron moves in the laser field, converting virtual transition into real and oscillating as the free electron should. It accumulates the phase given by the integral of its instantaneous energy $E(t'')$, performed between the moment of 'birth' in the continuum t' and the moment of observation t.

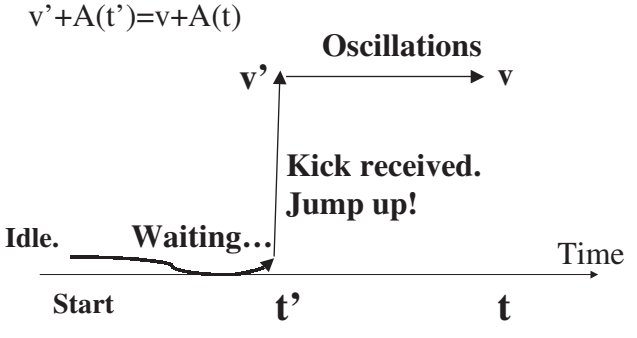

Figure 1. Graphical explanation of the transition amplitude $a_{\mathbf{v}}$. The electron is kicked into the continuum at time t' with velocity $\mathbf{v}'$, oscillates between t' and t, and acquires the velocity $\mathbf{v}$ at time t.

There are several major problems with this result, all stemming from the main approximation of the theory: to ignore the effect of the binding potential after t'.

(1) The kick at t' only begins the real transition to the continuum, which is affected by the interaction with the binding potential after t', neglected in the SFA. Thus, in the SFA the ionization amplitude can be quite different from its true value. The flaw can be fixed to some extent by using the limit of a constant electric field $\omega_L \to 0$. Tunnel ionization in a constant electric field is well known and can be described analytically for the Coulomb potential [4]. Comparing the SFA ionization rates in the tunneling limit of $\omega_L \to 0$ with actual tunneling rates, one can fix the incorrect pre-exponential factor the SFA gives, as described already by Keldysh [1].

(2) Propagation in the continuum is also different: the electron not only oscillates in the laser field, it also scatters off the atomic (molecular) core during these oscillations. Scattering causes transitions to new states $\mathbf{v}''$. Such transitions are not in any way present in equation (10).

The SFA result equation (10) is the first term in the expansion in powers of the binding potential. Scattering off the parent ion appears via higher-order terms, each new term corresponding to a larger number of electron–parent ion collisions. Unfortunately, this expansion, while being very appealing from the physical perspective, does not rigorously converge.

(3) The SFA is sensitive to gauge. We used the length gauge $\hat{V}_L(t) = -\mathbf{dF}(t)$. In the velocity gauge where $\hat{V}_L = -\hat{\mathbf{p}}\mathbf{A}$ the coordinate part of the propagator does not change: in this gauge the coordinate part of the plane wave $|\mathbf{p}\rangle$ stays the same between t' and t, while in the length gauge $|\mathbf{v}'\rangle \to |\mathbf{v}\rangle$. Physically, this is because in the velocity gauge $\hat{\mathbf{p}}$ refers to the conserved *canonical* momentum $\mathbf{P} = \mathbf{v} - \mathbf{A}(t)$ and not the *kinetic* momentum $\mathbf{v}$. This would not have led to any problems in the exact theory, i.e. if the electron had indeed been truly free all the time. But in the approximate theory this is not the case—the initial (ground) field-free state is not a free electron state, and no gauge-consistent phase enters it. *The result is that the SFA is not gauge invariant, which is really bad news for a theory*. In real life, observable physical effects do not depend on gauges.

However, the good news is that, when it comes to ionization rates, all these problems affect the pre-exponential term in the ionization amplitude but keep the main part, which is due to the fast oscillating exponent, intact. Having this in mind, we re-write the SFA amplitude with exponential accuracy, neglecting the matrix elements in front of the exponent:

$$\Psi(\mathbf{v}, t) \sim -i \int_0^t \mathrm{d}t' \exp(-iS_{\mathbf{v}}(t, t')), \tag{11}$$

where

$$S_{\mathbf{v}}(t, t') = \frac{1}{2}\int_{t'}^{t} \mathrm{d}t''[v_x - v_0 \sin\omega_L t + v_0 \sin\omega_L t'']^2 - I_p t' + \frac{v_\perp^2}{2}(t - t'). \tag{12}$$

Here $v_0 = F/\omega_L$ is the amplitude of the electron oscillation velocity and v_x and $v_\perp$ are the components of $\mathbf{v}$ along and perpendicular to the laser field, which we have assumed to be linearly polarized along the x axis. The vector-potential has been defined as

$$\mathbf{A}(t) = \mathbf{e}_x \frac{F}{\omega_L} \sin\omega_L t \equiv \mathbf{e}_x v_0 \sin\omega_L t, \tag{13}$$

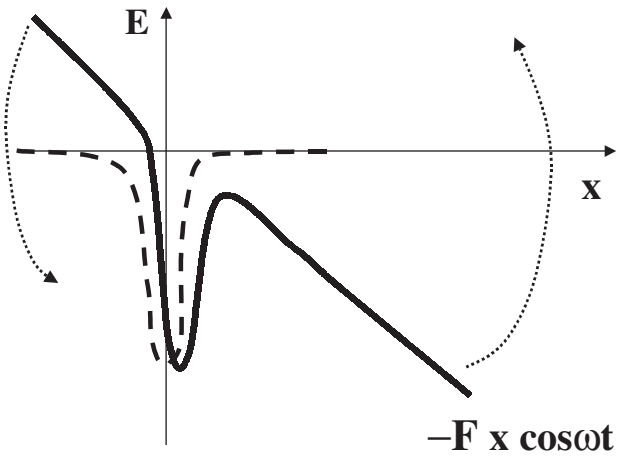

Figure 2. The solid line shows the potential created by the instantaneous laser field and the binding potential well. The dashed line shows the binding potential well on its own. Arrows show that the tails of the potential oscillate out of phase.

which means that the electric field is $\mathbf{F}(t) = -\mathbf{e}_x F \cos \omega_L t$ and the interaction with the laser field is $\hat{V}_L(t) = -\mathbf{dF}(t) = -qxF(t) = -xF \cos \omega_L t$ ($q = -1$). The minus in front of $\cos \omega_L t$ means that the electron moves to the right when $\cos \omega_L t > 0$, just as shown in figure 2.

4. Multiphoton and tunnel ionization: the peaceful co-existence

The SFA amplitude equations (11) and (12) can be used to derive rates of ionization in strong low-frequency fields. It also helps to answer the question of how the two different ionization mechanisms, tunneling and multiphoton, co-exist.

Before proceeding to formal mathematics, let us discuss physics first. The potential seen by an electron looks something like in figure 2. Two things must be mentioned.

(1) First, the potential well itself, in the classically allowed region, is being distorted and shaken every laser cycle, but only if the well has a reasonable size. *There is no distortion of the infinitely narrow and infinitely deep hole which is called the delta-function potential* and is a favourite toy of strong field theorists.

(2) Second, the barrier is oscillating up and down, opening a possibility for the electron to tunnel out every half-cycle. In principle, this is true for any laser frequency, intensity, etc. But whether the chance for tunneling would be used, and how, remains to be seen.

4.1. *Nearly classical ionization: climbing the vertical energy axis*

The two effects described above lead to two different ionization channels. The first ionization channel is due to periodic distortions of the potential well. In principle, it can be unrelated to tunneling: ionization may proceed mostly via the classically allowed region, as shown in figure 3. Let us call this the 'vertical' channel.

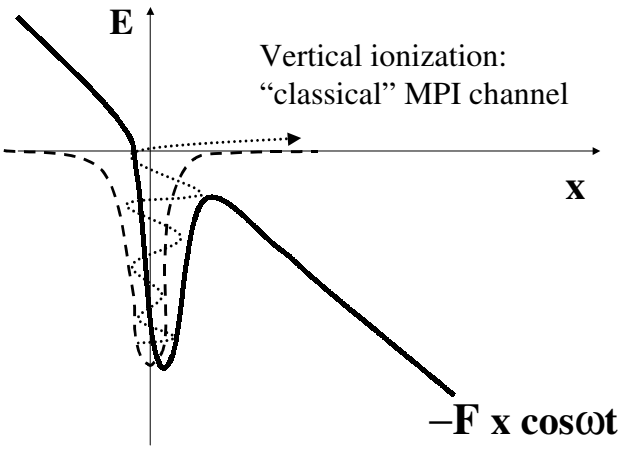

Figure 3. Vertical ionization channel: classical view of multiphoton ionization.

In the vertical channel the electron is 'heated' by the shaking walls of the potential well. Eventually, it gains enough energy to slip out of the well. Classical dynamics before the escape is likely chaotic. Even though the escape seems more likely when the barrier is maximally suppressed, dynamics could be such that the 'tail' of the potential might slam the electron right into the face when it was just about to roll over the barrier, closing the escape hatch and giving the electron enough energy to get out of the well as soon as the barrier is just lowered during the next laser cycle.

This picture is borrowed from the well-studied classical dissociation of diatomic molecules in the ground electronic state, induced by infrared (IR) laser fields. Mathematically, dissociation of a diatomic due to the interaction of the IR field with the permanent dipole moment looks very similar to ionization, except for the mass of the escaping particle. For heavy nuclei tunneling plays a much lesser role than for electrons and such 'classical' mechanism of escaping from the well can be easily separated from the tunneling contribution.

Further interaction of the escaped electron with the oscillating 'tail' of the potential $-Fx\cos\omega_L t$ leads to additional absorption of energy. This is a direct result of dropping the electron into the continuum at a certain phase of the laser field.

The sketch in figure 3 reminds us of the standard picture of multiphoton absorption—a vertical climb up the energy axis. The 'vertical' channel does not exhaust all multiphoton processes, it only deals with the motion within (or near) the classically allowed region. Now, let us address the most vital issue: is this ionization channel important?

Well, there is no such channel in short-range potentials, especially the delta-function-like. These latter can never be distorted, squeezed, etc. No classical-like vertical motion shown in figure 3 is possible. But this mechanism will certainly become more prominent as we increase the size of the well, *as long as the laser frequency is not too low compared to the electronic response time*. Indeed, if we distort the potential well on the time scale which is very long compared to the response time of the system, it will simply adjust to such distortions adiabatically. Therefore, in low-frequency fields and for ground states (small effective well size, fast

response time) such an ionization mechanism is not efficient, unless a resonance with some excited state is hit (which slows down the response time). Thus, a purely vertical channel is not important for IR laser frequencies and high I_p (i.e. fast response time $\sim 1/I_p$) atoms such as noble gases. This is why SFA works well for those, even in what is nominally the 'multiphoton' regime (see below).

Inefficiency of the vertical channel is very good news for the SFA. By virtue of its construction, the SFA explicitly neglects any effect of the binding potential on the electron evolution after it receives the first kick at t'. At this point the SFA loses any chance to include dynamics inside the well. By disposing of the well at t', the SFA is bound to deal with the dynamics of the tail of the initial wavefunction in the classically forbidden region. This is where the 'horizontal' ionization channel comes in.

4.2. *Deeply quantum ionization: the horizontal channel*

The 'horizontal' ionization channel explicitly uses the ability of the electron to tunnel through the barrier which is created every half-cycle. While the electronic wavefunction in the ground state adjusts to slow modifications of the well, its tail tries to leak out through the barrier which shows up every half-cycle. Depending on the frequency of the laser field, the barrier is either quasi-static, in which case simple tunneling formulas for a constant electric field can be used, or the barrier moves while the electron tunnels, leading to changes in the electron energy under the barrier. This is pictured in figure 4.

Usually, the question of whether or not the electron *can make it through the barrier* is identified with the relationship between some tunneling time τ, which we will define below, and the laser period. *This is a conceptual error*. The famous tunneling condition $\gamma \ll 1$, where the Keldysh parameter γ is

$$\gamma = \sqrt{I_p/2U_p}, \quad U_p = F^2/4\omega_L^2, \tag{14}$$

and U_p is the average energy of electron oscillations, can indeed be understood as $\omega_L \tau \ll 1$ [1]. It indeed means that the barrier does not move too much during

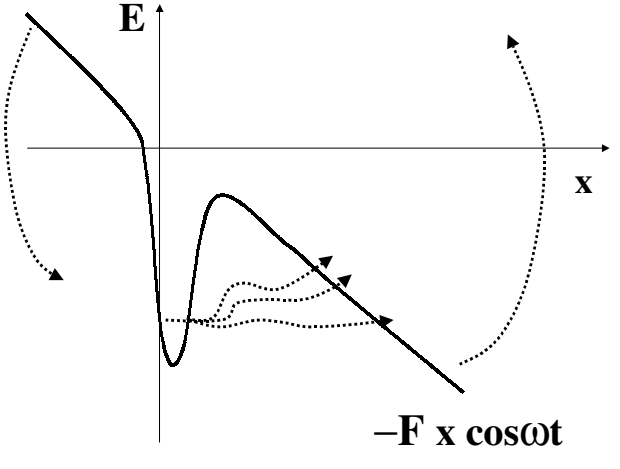

Figure 4. Tunneling ionization channel, with the possibility of changing the electron energy during tunneling due to the oscillation of the barrier (non-adiabatic tunneling).

tunneling. But this does not preclude tunneling when $\gamma > 1$—it only makes it more interesting. The tunneling component is still present in what is known as the 'multiphoton' regime $\gamma > 1$.

Let us begin with the tunneling time τ. It is a fairly complex notion, with many possible definitions depending on the physical effects and the observables one is interested in, see [5]. For our particular problem, the appropriate definition of the tunneling time has already been discussed by Keldysh [1]: it is the time it would take a classical particle to traverse the barrier pretending that the motion is classically allowed. Let us calculate this classical tunneling time τ, see that γ is indeed $\gamma = \omega_L \tau$, and then discuss the flaws of identifying tunneling with the famous condition $\gamma \ll 1$. Then, we will present a physical picture of what happens in the grey area of $\gamma \sim 1$ and support it with math.

For the binding energy I_p and a short-range potential, the velocity of the particle travelling through a triangular barrier created by the constant electric field changes as $v(t) = v_{max} - Ft$. Here $v_{max} = (2I_p)^{1/2}$ is the velocity at the entrance under the barrier. Setting $v(\tau) = 0$, we obtain the tunneling time τ:

$$\tau = \frac{v_{max}}{F} = \frac{\sqrt{2I_p}}{F}. \tag{15}$$

Now it is obvious that the famous Keldysh parameter γ is indeed $\gamma = \omega_L \tau$:

$$\omega_L \tau = \frac{\omega_L \sqrt{2I_p}}{F} = \sqrt{\frac{I_p}{2U_p}} = \gamma. \tag{16}$$

For $\gamma \ll 1$ we can treat the barrier as static while the electron moves through it. But does $\gamma > 1$ imply that no tunneling takes place? Of course not! An alternative, 'vertical' ionization channel, is *explicitly excluded* in SFA. Therefore, any ionization within SFA should involve tunneling, but for $\gamma > 1$ the barrier moves during it. What happens is simple: the electron absorbs energy while moving under the barrier, combining horizontal tunneling with vertical heating of the wavefunction's tail *inside the classically forbidden region*. If the energy goes up, the barrier becomes narrower and escapes easier. Thus, at $\gamma > 1$ tunneling acquires a strong non-adiabatic, vertical, component that eventually begins to dominate the horizontal motion of the wavefunctions's tail. But all this happens inside the classically forbidden region. Horizontal tunneling and vertical multiphoton absorption co-exist, ready to lend each other a helping hand. Now, we can turn to math.

4.3. *Non-adiabatic tunneling*

The total population accumulated in the continuum at time t is

$$W(t) = \int d\mathbf{v}\, |a_{\mathbf{v}}(t)|^2. \tag{17}$$

In SFA $a_{\mathbf{v}}(t) = \Psi(\mathbf{v}, t)$. Despite all the approximations, equations (11) and (12) are quite complicated and having to integrate over all $\mathbf{v}$ seems to just add to the pain. We will take an easy way out, aiming at getting the result only with exponential accuracy (a sensible thing to do when using SFA, which does not guarantee more anyway). We need to find out how much $W(t)$ gains during an interval δt just preceding t. For that, let us look at how $\Psi(\mathbf{v}, t)$, equations (11) and (12), is accumulated over time.

Equation (11) can be analysed using the saddle point method, which means that we have to look for the points where the phase $S_{\mathbf{v}}(t, t')$ has zero derivative with respect to the variable of integration t'. The integral equation (11) is accumulated near these points, with the contribution from each proportional to the value of the integrand at the saddle point.

Using equation (12), we see that the saddle points t' are given by

$$\frac{1}{2}(v_x - v_0 \sin \omega_{\mathrm{L}} t + v_0 \sin \omega_{\mathrm{L}} t')^2 + \left(I_{\mathrm{p}} + \frac{1}{2} v_{\perp}^2\right) = 0. \tag{18}$$

The first thing to note is that creating electrons with non-zero $v_{\perp}$ is the same as having higher I_{p}. Higher I_{p} means harder ionization. Thus, the integrand over $dv_{\perp}$ in equation (17) is peaked at $v_{\perp} = 0$ and to get the ionization rate with exponential accuracy we can set $v_{\perp} = 0$. This changes equation (18) into

$$(v_x/v_0 - \sin \omega_{\mathrm{L}} t + \sin \omega_{\mathrm{L}} t')^2 + \gamma^2 = 0. \tag{19}$$

What about v_x? Physically, since we are interested in the population that has just appeared in the continuum, it is reasonable to assume that v_x/v_0 is negligible. Let us see what equation (19) has to say about it.

Firstly, solutions of equation (19) are always complex: all t' will have an imaginary part due to the γ^2 term. Complex time is consistent with motion in the classically forbidden region, i.e. tunneling. In SFA all ionization, no matter what γ, is always rooted in tunneling.

Secondly, real solutions t' would have appeared if we were to neglect γ^2 in equation (19). The resulting equation $v_x/v_0 + \sin \omega_{\mathrm{L}} t = \sin \omega_{\mathrm{L}} t'$ is nothing but the condition on t' that allows the electron to be *born with zero velocity at* t', gaining v_x by the moment t. Thus, if we are interested in the population that has just appeared in the continuum, with $\mathrm{Re}(t')$ as close to t as possible, we should indeed set $v_x/v_0 = 0$. With exponential accuracy, we should get the recent gain in the continuum population $W(t)$ by looking at $\Psi(\mathbf{v}, t)$ for $\mathbf{v} = 0$. Thus, we have to deal with a much simpler saddle point equation

$$(\sin \omega_{\mathrm{L}} t - \sin \omega_{\mathrm{L}} t')^2 + \gamma^2 = 0. \tag{20}$$

For the saddle point closest to t, denoted as t'_0, $\mathrm{Re}(t'_0) \approx t$. Other t'_n are separated from t'_0 by the integer number of cycles, $t'_n = t'_0 - 2\pi\omega_{\mathrm{L}}^{-1} n$, integer $n \geq 1$. The physical meaning of these saddle points is as follows.

(1) The contribution of the saddle point t'_0 to $\Psi(\mathbf{v}, t)$ describes the population that has just appeared in the continuum; the complex t'_0 is the moment when the electron enters the classically forbidden region under the barrier.

(2) Contributions of the saddle points t'_n, $n \geq 1$, describe the population created in the continuum one or more laser cycles ago; the corresponding phases $S_{\mathbf{v}}$, equation (12), contain contributions from the free electron motion in the continuum.

Since we are interested in the most recent addition to the ionization amplitude, we should only take into account the contribution $\delta\Psi(t)$ of the single saddle point $t'_0(t)$.

This is a big relief. We do not have to calculate the integral over $d\mathbf{v}$, searching for all saddle points for all $\mathbf{v}$. We can set $v = 0$, take a single saddle point, and worry about possible corrections to pre-exponential factors later.

The saddle point contribution is $\delta\Psi(v=0,t) \propto \exp[-iS_{v=0}(t, t_0'(t))]$. Denoting $S_{v=0}(t, t_0'(t)) \equiv S_0$ and writing $S_0 = \mathrm{Re}(S_0) - i\,\mathrm{Im}(S_0)$, for the ionization rate we will have

$$\Gamma(t) \propto \exp[-2\,\mathrm{Im}(S_0)]. \tag{21}$$

The complex phase S_0 is

$$S_0 = \frac{v_0^2}{2}\int_{t'}^{t} \mathrm{d}t'' \,[\sin\omega_{\mathrm{L}}t - \sin\omega_{\mathrm{L}}t'']^2 - I_{\mathrm{p}}t', \tag{22}$$

and $t' = t_0'(t)$ is given by equation (20). Calculation can be carried out for any $\omega_{\mathrm{L}}t$, but for simplicity we shall look at the maxima of the electric field, $\omega_{\mathrm{L}}t = \pi K$ (in the tunneling regime $\gamma \ll 1$ the rate is peaked near $\omega_{\mathrm{L}}t = \pi K$, while in the deep multiphoton regime $\gamma \gg 1$ it makes no difference which phase $\omega_{\mathrm{L}}t$ is chosen).

For $\omega_{\mathrm{L}}t = \pi K$ the saddle point equation is $\sin^2\omega_{\mathrm{L}}t' + \gamma^2 = 0$. Setting $t' = \pi K/\omega_{\mathrm{L}} + i\tau$, we get

$$\sinh\omega_{\mathrm{L}}\tau \equiv \frac{e^{\omega_{\mathrm{L}}\tau} - e^{-\omega_{\mathrm{L}}\tau}}{2} = \pm\gamma, \tag{23}$$

and the phase S_0, after writing the integration variable as $t'' = \pi K/\omega_{\mathrm{L}} + i\xi$, is

$$S_0 = -iI_{\mathrm{p}}\tau + i\frac{v_0^2}{2}\int_0^{\tau} d\xi \sinh^2\omega_{\mathrm{L}}\xi. \tag{24}$$

As often the case with saddle point equations, equation (23) has two solutions. Positive τ gives exponentially small $\exp(-iS_0)$ (see equation (24)), and negative τ gives an exponentially large result. Which saddle point to choose? Physics suggests that ionization should be described by an exponentially small rate (think about the tunneling limit of $\omega_{\mathrm{L}} \to 0$). One can show that, mathematically, this is indeed the correct choice.

For small $\gamma \ll 1$, from equation (23) we have our familiar tunneling time $\tau = \gamma/\omega_{\mathrm{L}}$. Using equation (24), in this limit we get $S_0 = -i(I_{\mathrm{p}}\tau - 2U_{\mathrm{p}}\gamma^2\tau/3) = -i(2/3)I_{\mathrm{p}}\tau$ and hence the rate is

$$\Gamma = X\exp[-2\,\mathrm{Im}(S_0)] = X\exp\left(-\frac{4}{3}I_{\mathrm{p}}\tau\right) = X\exp\left(-\frac{2(2I_{\mathrm{p}})^{3/2}}{3F}\right), \tag{25}$$

where X is an unknown factor. Equation (25) is the same as for tunneling through a triangular barrier formed by a constant electric field and a short-range potential. The factor X can now be fixed by using the correct answer for tunneling through the Coulomb barrier [4, 6]; it is reasonable to use the same X not only for $\gamma \ll 1$, but also for $\gamma \geq 1$.

For large γ the tunneling time τ changes, and quite significantly. In the limit $\gamma \gg 1$, equation (23) yields $\tau \approx \ln(2\gamma)/\omega_{\mathrm{L}}$ and

$$\mathrm{Im}(S_0) \approx \frac{I_{\mathrm{p}}}{\omega_{\mathrm{L}}}\ln 2\gamma. \tag{26}$$

This means that the formally exponential dependence turns into the power law

$$\Gamma(t) = X\exp(-2\,\mathrm{Im}[S]) = X(2\gamma)^{-2N} \propto F^{2N}, \tag{27}$$

where $N = I_{\mathrm{p}}/\omega_{\mathrm{L}}$ is the number of photons required to reach the continuum threshold. The fact that it is not an integer is a result of considering dynamics

during the sub-cycle: we have not waited long enough to figure out that the field is periodic and resolve the photon energy.

Thus, in SFA, electrons are always tunneling, but at $\gamma > 1$ they are heated up while moving under the barrier, leading to multiphoton absorption from under the potential barrier.

5. Electron wavepacket after tunneling

In this section, we look at the anatomy of the electronic wavepacket as it emerges from under the potential barrier. For simplicity, we shall focus on the constant electric field. Numerics [12] show that our conclusions are applicable not only for $\gamma < 1$ (which is not surprising), but also in the intermediate regime of $\gamma \sim 1$.

Why bother with a seemingly academic question? Besides mere curiosity, our motivation lies in the desire to replace quantum simulations in strong laser fields with classical. Sometimes it is the only tractable approach, especially when other electrons are involved, and it is hard to deal with tunneling classically. It seems reasonable to take an eclectic route: solve the tunneling problem quantum-mechanically, find the shape of the electronic wavepacket after it shows up in the classically allowed region, and then replace it with a swarm of trajectories. Classical approaches work very well in strong fields, and can be further improved by using the so-called semi-classical initial value representation methods (see, e.g. [7, 8] for the general approach; for applications to strong fields see, e.g., [9–11]).

To find the shape of the wavepacket after tunneling, we have to look at $\Psi(\mathbf{v})$ for non-zero $\mathbf{v}$. In the limit of a constant electric field $\omega_L \to 0$ the SFA phase equation (12) is

$$S_{\mathbf{v}}(t, t') = \frac{1}{2}\int_{t'}^{t} \mathrm{d}t'' \, [v_x - F(t - t'')]^2 + \frac{v_\perp^2}{2}(t - t') - I_p t'. \tag{28}$$

Introducing the new integration variable $t_D = t - t'$, the time delay between the electron 'birth' at t' and the moment of observation t, we get

$$\Psi(\mathbf{v}, t) \sim -i \exp[iI_p t] \int_0^t \mathrm{d}t_D \exp(-iS_{\mathbf{v}}(t_D)), \tag{29}$$

where

$$S_{\mathbf{v}}(t_D) = \frac{1}{2}\int_0^{t_D} \mathrm{d}t'' \, [v_x - Ft'']^2 + I_p t_D + \frac{v_\perp^2}{2} t_D, \tag{30}$$

and the integration variable in S_v has been tweaked: $t - t'' \to t''$. The term $\exp(iI_p t)$ gives a global phase and is dropped below.

5.1. *Transverse velocity distribution*

First, let us deal with the wavepacket dependence on $v_\perp$. Setting $v_x = 0$, we get

$$\Psi(v_\perp, t) \sim -i \int_0^t \mathrm{d}t_D \exp\left[-i\left(\frac{F^2}{6} t_D^3 + I_p t_D + \frac{v_\perp^2}{2} t_D\right)\right]. \tag{31}$$

Let us assume that the field has been on for a long time and take the maximum delay time $t \to \infty$. This yields a steady-state distribution $\Psi(v_\perp)$. The saddle point of equation (31) is given by

$$\frac{F^2}{2} t_{\mathrm{D}}^2 + I_{\mathrm{p}} + \frac{v_\perp^2}{2} = 0. \tag{32}$$

For small $v_\perp^2/2 \ll I_{\mathrm{p}}$ the saddle point is

$$t_{\mathrm{D}}^{(0)} = -i\tau = -i\frac{\sqrt{2I_{\mathrm{p}}}}{F}. \tag{33}$$

The 'minus' sign $(-i)$ chosen for $t_{\mathrm{D}} = t - t'$ is consistent with the positive sign $(+i)$ chosen for t' in the previous section. Calculating the integrand at the saddle point, we see that, after tunneling, the wavepacket has a simple Gaussian dependence on $v_\perp$:

$$\Psi(v_\perp) = \Psi(0) \exp\left[-\frac{v_\perp^2}{2}\tau\right]. \tag{34}$$

The wavepacket width is determined by the tunneling time and reminds us of the energy–time uncertainty relationship. It suggests that the tunneling time can also be associated with the uncertainty in the moment of time at which the wavepacket appears from under the barrier.

To check the analytical result, equation (34), we have performed *ab initio* numerical simulations for a model soft-core Coulomb potential

$$V_{\mathrm{A}}(x, y) = -\frac{1}{\sqrt{x^2 + y^2 + 0.25}} \tag{35}$$

in the presence of the electric field $F(t) = -F\cos\omega_{\mathrm{L}} t$ with $\omega_{\mathrm{L}} = 0.057$ a.u. (corresponding to $\lambda = 800$ nm wavelength) and the peak electric field $F = 0.14$ a.u. (intensity $I = 6.9 \times 10^{14}\,\mathrm{W/cm^2}$). Propagation was done for one half-cycle from $\omega_{\mathrm{L}} t = -\pi/2$ to $\omega_{\mathrm{L}} t = \pi/2$. For this model atom $I_{\mathrm{p}} = 0.65$ a.u. and the Keldysh parameter is $\gamma = 0.46$.

The resulting wavepacket $\Psi(\mathbf{v}, t = \pi/2\omega_{\mathrm{L}})$ is shown in figure 5 in the velocity space. Figure 5(*a*) shows $|\Psi(v_x, v_y)|$ as a colour-coded plot in log scale, with different orders of magnitude corresponding to different colours (shades of grey). Figure 5(*b*) shows the transverse cross-section of the wavepacket taken along the dashed line in figure 5(*a*). The cross-section corresponds to that part of the wavepacket which tunneled out near the peak of the field $\omega_{\mathrm{L}} t = 0$. The Gaussian fit $\Psi(v_y) \propto \exp(-4.6 v_y^2)$ to the exact numerical data is excellent. The numerically determined value, 4.6, is very close to the analytical prediction, $\tau/2 = 4.1$. Deviations are due to the focusing by the Coulomb potential.

5.2. *Longitudinal distribution and the Husimi representation*

Identifying the wavepacket dependence on v_x is much harder. The crucial difficulty stems from the fact that the laser field accelerates the electron while it tunnels out. The velocity distribution along the field is changed continuously during tunneling. This is in stark contrast with the transverse velocity distribution which is unaffected by the laser field and can be easily distilled out. Uncertainty in the moment of tunneling, which is responsible for the uncertainty in the initial velocity, also means that it is virtually impossible to separate the initial velocity

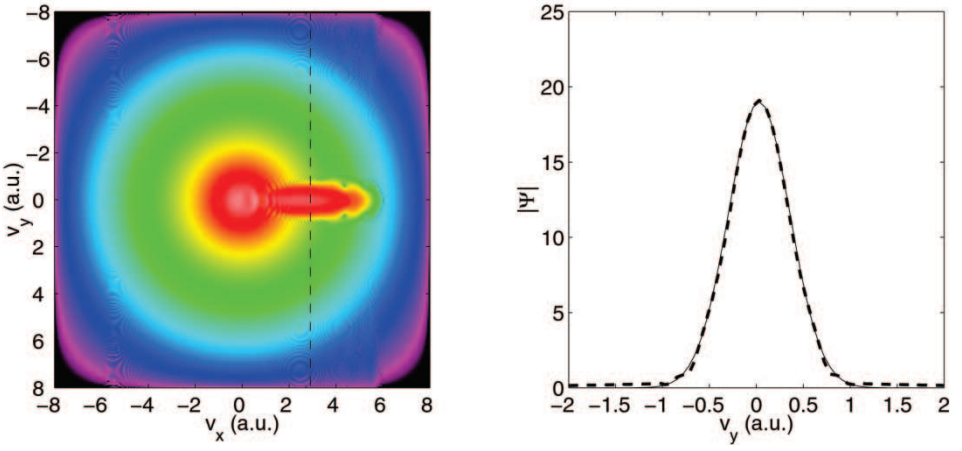

Figure 5. (*a*) Electronic wavepacket after tunneling from a two-dimensional soft-core potential, shown in the velocity space as a colour-coded (online) or grey-scale coded (in print) logarithmic plot of $\Psi(v_x, v_y)$. Different colours correspond to different orders of magnitude of $|\Psi(v_x, v_y)|$, in the order white, red, yellow, green, light blue, dark blue and pink. (*b*) Transverse section of the wavepacket with a Gaussian fit.

distribution from the distortions caused by the electric field during this temporal uncertainty.

Nevertheless, let us attempt to address this problem. Setting $v_\perp = 0$ in equations (29) and (30), we get

$$\Psi(v_x) \sim -i \int_0^\infty \mathrm{d}t_\mathrm{D}\, \exp\left[-i\left(\frac{F^2}{6} t_\mathrm{D}^3 - \frac{v_x F}{2} t_\mathrm{D}^2 + \frac{v_x^2}{2} t_\mathrm{D} + I_\mathrm{p} t_\mathrm{D}\right)\right], \tag{36}$$

and the key difference from the transverse case is the $v_x F t_\mathrm{D}^2/2$ term, which changes the saddle point equation to

$$\frac{1}{2}(F t_\mathrm{D} - v_x)^2 + I_\mathrm{p} = 0. \tag{37}$$

It is very tempting to say that we are looking for small longitudinal velocities, drop v_x from equation (37) and use the exact same tunneling time $t_\mathrm{D} = -i\tau = -i(2I_\mathrm{p})^{1/2}/F$ for the effective moments of birth. If we were to do that and pull the phases proportional to v_x out of the integral in equation (36), at the point $t_\mathrm{D} = -i\tau$, we would have obtained the following dependence on v_x:

$$\Psi(v_x) = \Psi(0) \exp\left[-\frac{v_x^2}{2}\tau - i\frac{v_x F}{2}\tau^2\right] = \Psi(0) \exp\left[-\frac{v_x^2}{2}\tau - i v_x x_\mathrm{e}\right]. \tag{38}$$

While the first term in the exponent describes the same Gaussian shape, the second term corresponds to the shift of the wavepacket centre to the exit of the tunnel $x_\mathrm{e} = F\tau^2/2 = I_\mathrm{p}/F$, exactly the position where the electron is supposed to emerge from under the barrier (neglecting the binding potential, of course).

While this seems a reasonable answer, it looks a bit odd that immediately after tunneling the wavepacket has exactly the same chance to have negative velocity $v_x < 0$ as it has to have positive velocity $v_x > 0$. We would have expected that after

tunneling the distribution would favour trajectories running away from the barrier.

What if we were to use the exact saddle point given by equation (37)? The exact solution of equation (37) is

$$t_{\mathrm{D}} = \frac{v_x}{F} - i\tau. \tag{39}$$

Apart from tunneling time $-i\tau$, the real part of this time delay corresponds precisely to the time it takes an electron born with *zero initial velocity* to accelerate to v_x in the electric field F. Thus, just as noted at the beginning of this subsection, mathematics is trying to cheat us, offering an answer we are not looking for. Instead of giving us an amplitude to have v_x at 'birth', it gives us an amplitude of tunneling out with *zero* velocity at an appropriate earlier time and then accelerating to v_x.

Thus, straightforward application of the saddle-point approach, so successful in the case of a transverse distribution, seems to stumble in the longitudinal case. Rigorously, $\Psi(v_x)$ is dominated by tunneling with $v_x = 0$ at an earlier moment of time. The result, equation (38), although plausible, so far is too much on a hand-waving side. Is there something else we can do to shed light on the shape of the wavepacket?

Recall that our motivation was to find a reasonable classical ensemble to reproduce quantum dynamics after tunneling. The best place to draw parallels between quantum and classical ensembles is phase space. One of the most frequently used quantum phase-space-type distributions is the Wigner function [13]. The Wigner representation has already been used in [14] exactly for our problem: to look at the wavepacket during tunneling. However, here we will use different phase-space representation of our wavepacket: decomposition into the Gaussian basis. Such decomposition turns out to be the most adequate phase-space representation for the semiclassical propagators (see, e.g. [7, 8]). The corresponding phase-space distribution is

$$H(v_0, x_0) = \langle G(v_x|v_0, x_0)|\Psi(v_x)\rangle, \tag{40}$$

where, in the velocity representation, the Gaussian wavepacket centred at the point (v_0, x_0) in the phase space is

$$G(v_x|v_0, x_0) \propto \exp\left[-\frac{(v_x - v_0)^2}{2}\tau - iv_x x_0\right]. \tag{41}$$

The width of the Gaussian wavepacket is chosen to correspond to the tunneling time τ. The Husimi-type representation, equation (40), will (i) emphasize the artifacts caused by the interference of quantum trajectories exiting the tunnel with different velocities at different times and (ii) show how these artifacts disappear as one moves away from the barrier.

Before calculating $H(v_0, x_0)$ numerically, let us look at equation (36) again. We can re-write it exactly as

$$\Psi(v_x) \sim -i\exp\left[-i\left(\frac{v_x^3}{6F} + x_{\mathrm{e}}v_x\right)\right] \times \int_0^\infty dt_{\mathrm{D}}\, \exp\left[-i\frac{1}{6F}\left((Ft_{\mathrm{D}} - v_x)^3 + x_{\mathrm{e}}(Ft_{\mathrm{D}} - v_x)\right)\right]. \tag{42}$$

Introducing dimensionless velocity $u = v_x/(2I_p)^{1/2}$ and a new integration variable $u' = [Ft_D - v_x]/(2I_p)^{1/2}$, we obtain

$$\Psi(v_x) \sim -i\tau \exp\left[-i\kappa\left(\frac{u^3}{3}+u\right)\right]\int_{-u}^{\infty} du' \exp\left[-i\kappa\left(\frac{u'^3}{3}+u'\right)\right],$$
$$v_x = u\sqrt{2I_p}, \tag{43}$$

where $\kappa \equiv I_p(2I_p)^{1/2}/F$. The result contains only a single parameter κ, which also controls tunneling (equation (25), and can be re-written as $\Gamma = X\exp(-4\kappa/3)$). Typically, $\kappa \gg 1$.

For sufficiently large positive u the lower limit of the integral equation (43) $(-u)$ can be replaced with $-\infty$. The integral term looses its u dependence and the wavefunction converges to a stationary solution of the Schroedinger equation in a constant electric field: an outgoing wave with energy $-I_p$ and zero velocity at $x = x_e = I_p/F$, accelerating away from the origin. In the velocity domain, such a solution is indeed $\Psi(v_x) \propto \exp(-i[v_x^3/6F + x_e v_x])$. Its Husimi-type representation is centred around the classical trajectory that starts at x_e with zero velocity.

Figure 6 shows numerical calculations of $H(v, x)$ for $\Psi(v_x)$ given by equation (43). Classical trajectory which starts at x_e with zero velocity is shown with a thick solid line. Figure 6 clearly demonstrates that, sufficiently far from the tunnel, the phase-space distribution is indeed centred around this trajectory. The same conclusion was reached in [14] for the Wigner distribution.

Even for small u the integral in equation (43) is clearly asymmetric: for $u > 0$ the real part of the saddle point $u'_0 = -i$ is between the limits of integration, while

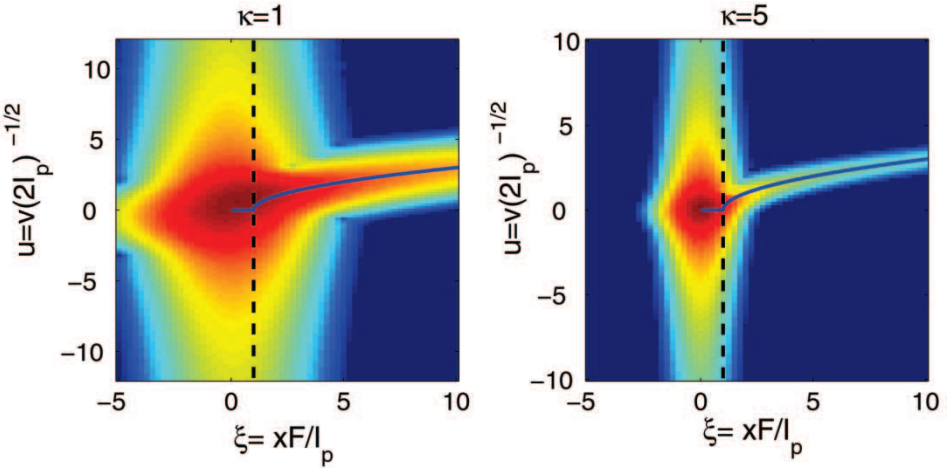

Figure 6. Hismi-type distributions $H(v, x)$ of $\Psi(v_x)$, colour-coded (online) or grey-scale coded (in print) on a log scale, as a function of the dimensionless coordinates $\xi = x/x_e = xF/I_p$ and $u = v/(2I_p)^{1/2}$, for different values of the parameter $\kappa = I_p(2I_p)^{1/2}/F$. Different colours correspond to different orders of magnitude of $|H(v, x)|$, in the order red, yellow, light blue, blue, dark blue. The left panel is for $\kappa = 1$ and the right panel is for $\kappa = 5$. The vertical line marks the exit from the tunnel, which is always at $\xi = 1$. The solid line at $\xi > 1$ is a classical trajectory which starts with zero initial velocity. The solid line at $0 < \xi < 1$ extentds it into the classically forbidden region, where the main peak reflects the reservoir of the population in the groud state.

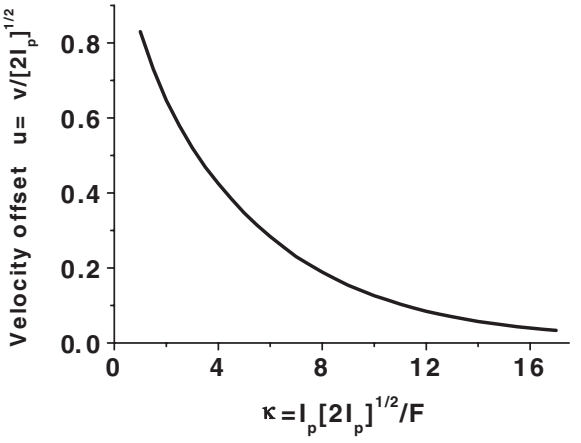

Figure 7. Velocity offset δv of the centre of the distribution $H(v, x)$ at the exit from the tunnel $x = x_e = I_p/F$, in units of $\delta u = \delta v/(2I_p)^{1/2}$, as a function of the parameter $\kappa = I_p(2I_p)^{1/2}/F$.

for $u < 0$ the real part $\mathrm{Re}\, u_0' = 0$ moves outside the integration limits, making negative u less probable and reflecting electron acceleration to positive velocities while tunneling. This asymmetry is very apparent in figure 6 already at the exit from the tunnel ($\xi = 1$). Asymmetry results in the shift δu of the maximum of the phase-space distribution to positive u (see also [14]).

The velocity offset δu decreases with increasing κ, i.e. as the barrier becomes larger and harder to penetrate. This is visible already in figure 6. Figure 7 shows the offset as a function of κ, and the characteristic dependence is on $\kappa^{-1/3}$.

The apparent velocity offset $\delta u = \delta v/(2I_p)^{1/2}$ at the exit from the tunnel is an 'artifact' of the interference discussed above. If we had a non-zero velocity in a classical sense, the peak of the Husimi distribution would have stayed above the classical trajectory (solid line in figure 6) by the exact same value δu, at all distances $\xi = x/x_e$. The offset results from the continuous stream of population coming from the ground state (note that equation (43) neglects the depletion of the ground state which acts as an infinite reservoir). Extending the classical trajectory from $\xi \geq 1$ into the region under the barrier at best corresponds to the horizontal line in figure 6, forming a cusp at $\xi = 1$. Quantum distribution smoothes this cusp.

We can summarize the discussion in this subsection as follows: near the exit from the tunnel, even in the classically allowed region, quantum dynamics noticeably deviates from classical. No classical ensemble can reproduce it perfectly. However, the deviation disappears as the wavepacket moves away from the barrier. According to figures 6 and 7 the most adequate way to represent a quantum distribution with a classical ensemble is still to centre it around the classical trajectory starting with $u_0 = 0$ at $\xi = 1$. Then the classical ensemble will be able to merge with the quantum wavepacket at $\xi \gg 1$. At $\xi \gg 1$ the phase-space distribution in figure 6 contains velocities both smaller and larger than those for the classical trajectory starting with $u_0 = 0$ at $\xi = 1$. To represent this classically, immediately after tunneling the classical distribution should contain both negative and positive velocities and have coordinates $\xi < 1$ and $\xi > 1$. The distribution equation (38) meets these criteria.

6. Conclusions

Our goal was to provide an introductory overview, focusing on (i) the dynamics of the electron transition to the continuum in strong IR laser fields, and (ii) the shape of the electron wavepacket as it appears in the continuum. At least one of us (M.I.) was driven by the desire to find simple and clear answers to basic questions about strong field ionization that troubled him since his university years, and put these answers in writing. The occasion of this special issue dedicated to the birth of attosecond science is appropriate.

We have described the physics behind a smooth transition of 'horizontal' tunneling ionization at $\gamma \ll 1$ into the 'vertical' multiphoton ionization at $\gamma \gg 1$, and demonstrated that these two channels do not exclude each other. On the contrary, they can very well co-exist peacefully in the 'grey' area of $\gamma \sim 1$, where their combination leads to what can be best called 'non-adiabatic tunneling'.

Discussing the shape of the electronic wavepacket as it emerges from the potential well and appears in the continuum, we should stress several things. For the transverse distribution, the answer is very clear: tunneling provides a Gaussian filter for the initial bound state of the electron. The width of the filter is associated with the tunneling time. For the longitudinal distribution, the picture is spoiled by the continuous acceleration in the electric field during the (uncertain time of) emergence from under the barrier. It leads to the interference of the just starting 'quantum trajectory' with those started earlier with lower velocities. Velocity offset of the electron exiting the tunnel can be identified as the result of this interference, and it disappears as the electron moves away from the barrier.

Our discussion has completely neglected the initial shape of the bound state, which will inevitably be reflected in the outgoing wavepacket. Looking at equation (10), it seems very reasonable to complement the Gaussian shapes, equations (34) and (38), with the Fourier transform of the initial state skewed along the laser polarization:

$$\delta\Psi(\mathbf{v}) \propto \langle \mathbf{v}|x\Phi_{\mathrm{i}}\rangle \exp\left[-\frac{v^2}{2}\tau - i\mathbf{v}\mathbf{x}_{\mathrm{e}}\right], \tag{44}$$

where $\mathbf{x}_{\mathrm{e}}$ is the exit from the tunnel.

Acknowledgements

At various stages of this work we have greatly benefited from comments, suggestions and discussions with W. Becker, A. Scrinzi, and F. Krausz. M.I. is very grateful to both the Vienna group at the Photonics Institute and the Femtosecond group at NRC for valuable inputs during his lectures on the subject. M.I. and M.S. acknowledge financial support from an NSERC discovery grant to M.I. and from the NRC graduate student supplement program to M.S. M.I. and O.S. acknowledge the financial support of the NSERC International Opportunity Fund through the Canadian–Russian Photonics Network. M.I. acknowledges support of the visiting professorship at the Max-Plank-Institute.

References

[1] KELDYSH, L. V., 1964, *Zh. eksp. teor. Fiz.*, **47,** 1945 [English translation: 1965, *Soviet Phys. JETP*, **20,** 1307].

[2] Reiss H. R., 1980, *Phys. Rev.* A, **22,** 1786; see also REISS H. R., 1992, *Prog. quant. Electron.*, **16,** 1.

[3] Faisal, F. H. M., 1973, *J. Phys.* B, **6,** L89.
[4] Landau, L. D., and Lifshitz E. M., 1981, *Quantum Mechanics: Non-Relativistic Theory*, 3rd edn (London: Butterworth–Heinemann).
[5] Steinberg, A. M., 1995, In *Fundamental Problems in Quantum Theory*, edited by D. M. Greenberger and A. Zeilinger, *Ann. N.Y. Acad. Sci.*, **755,** 900.
[6] Delone, N. B., and Krainov, V. P., 1994, *Multiphoton Processes in Atoms* (Berlin: Springer).
[7] Herman, M. F., and Kluk, E., 1984, *Chem. Phys.*, **91,** 27.
[8] Kay, K. G., 1994, *J. chem. Phys.*, **100,** 4432.
[9] Van De Sand, G., and Rost, J. M., 1999, *Phys. Rev. Lett.*, **83,** 524; *ibid*, 2000, *Phys. Rev.* A, **62,** 053403.
[10] Grossmann, F., 2000, *Phys. Rev. Lett.*, **85,** 903.
[11] Spanner, M., 2003, *Phys. Rev. Lett.*, **90,** 233005.
[12] Scrinzi, A., unpublished results.
[13] Schleich, W., 2001, *Quantum Optics in Phase Space* (Weinheim, Germany: Wiley–VCH).
[14] Czirjak, A., Kopold, R., Becker, W., Kleber, M., and Schleich, W. P., 2000, *Optics Commun.*, **179,** 29.